CHINESE OPTICS LETTERS

Vol. 19, No. 7 | July 2021

Experimental observation of transient mode-locking in the build-up stage of a soliton fiber laser

Yinqi Wang (王殷琪)[1], Xiaoyue Wang (王小月)[1], Junsong Peng (彭俊松)[1], Ming Yan (闫 明)[1,2*], Kun Huang (黄 坤)[1,2**], and Heping Zeng (曾和平)[1,2,3]

[1] State Key Laboratory of Precision Spectroscopy, East China Normal University, Shanghai 200062, China

[2] Chongqing Institute of East China Normal University, Chongqing 401147, China

[3] Jinan Institute of Quantum Technology, Jinan 250101, China

*Corresponding author: myan@lps.ecnu.edu.cn

**Corresponding author: khuang@lps.ecnu.edu.cn

Received October 21, 2020 | Accepted December 5, 2020 | Posted Online March 23, 2021

In this paper, we demonstrated a series of short-living mode-locking (ML) states (each lasting a few to a hundred microseconds) that happened before a fiber laser reached a steady ML state. With time-stretched dispersion Fourier transform spectroscopy, a rich diversity of transient multi-pulse dynamics were revealed spectrally and temporally. As a result, we found that the formation of the short-living ML states was related to abundant pump power, and their decaying evolution dynamics were possibly governed by gain depletion and recovery. Our results revealed unexpected transient lasing behaviors of a soliton laser and thus might be useful to understand the complex dynamics of mode-locked lasers.

Keywords: mode-locking; soliton; fiber laser.

DOI: 10.3788/COL202119.071401

1. Introduction

Solitons in fiber lasers, a consequence of balanced intra-cavity nonlinearity and dispersion, have attracted much attention owing to their unique features of preserving their temporal and spectral shapes over propagation distances and to the wide application scope, ranging from optical communications to laser metrology and material processing[1–10]. Recently, the advance of the time-stretched dispersion Fourier transform (TS-DFT) spectroscopy has opened up new opportunities for revealing the underlying mechanisms of transient phenomena inside soliton lasers[5–13]. This technique builds a bridge between the temporal and spectral domains of ultrashort pulses, simply by stretching them in a dispersive medium, e.g., a piece of fiber. Together with a fast detector and an oscilloscope, the spectrum of a single pulse can be measured at a refresh rate as high as the pulse repetition rate, e.g., 90 MHz in Ref. [7]. By virtue of this fast detection technique, a number of intriguing phenomena have been observed in real time, such as dissipative rogue waves[14], soliton explosions[15–17], soliton rains[18], and breather-wave molecules[19].

Worthy of note is that many of these investigations emphasized the build-up stage of a mode-locked laser, where unpredicted soliton complexes thrive, and their dynamics have proven informative to the understanding of the soliton formation and interactions[7–13]. For instance, in Ref. [9], a soliton laser was found undergoing several stages, including raised relaxation oscillation (RO) in the form of growing laser spikes, *Q*-switched mode-locking (Q-ML) with strong modulations of pulse energy, and beating dynamics featuring transient spectral interference patterns, before entering a steady state of mode-locking (ML). In another case[10], solitons directly arising from *Q*-switching instead of RO have been observed. For soliton molecules (SMs), the build-up processes could be more complicated, where four-wave mixing (FWM) induced spectra, transient single-soliton states, and transient bound states might be involved[11]. Also, the studies of a new type of SMs (i.e., intermittent-vibration SMs[12,13]) have shown several nonlinear stages, including ML, soliton splitting, and soliton interactions, involved in the formations of the SMs. On the one hand, these works that highlight the importance of real-time temporal and spectral measurements have led to new perspectives for the transient properties of nonlinear optical systems. On the other hand, the onset dynamics in varied laser systems have shown a rich soliton diversity, which certainly calls for further investigations both theoretical and experimental.

In this paper, we investigated the build-up dynamics of a self-started soliton fiber laser with TS-DFT. We found a variety of short-lived pulsing states formed before the laser entered a steady soliton state. This is different from previous

demonstrations where RO, beating dynamics, and Q-switching (or Q-ML) were involved in the build-up stage of an ML laser[5–19]. Here, each transient pulsing state presented a complete picture of the formation, evolution, decay, and annihilation of the pulses. Furthermore, we found the decaying behavior of each pulsing state was governed by gain depletion and recovery in the fiber cavity. Also, the formation of these transient ML states was possibly attributed to redundant pump power or excess energy inside the cavity. Since such kinds of transient ML states with rich multi-pulse dynamics have not been well explored yet, we believe that our findings would contribute to the fields of optical solitons and fiber lasers.

2. Experimental Setup

Our experimental setup is shown in Fig. 1. The output of a soliton fiber laser was investigated. The fiber cavity contained a semiconductor saturable absorber mirror (SESAM), a piece of 0.8-m-long erbium-doped fiber (Er80-4/125-HD-PM, Liekki), and 1.2 m of polarization-maintaining fiber (PMF, dispersion of $-25\,\mathrm{ps}^2/\mathrm{km}$ at 1550 nm). The net intra-cavity dispersion was estimated to be $-0.014\,\mathrm{ps}^2/\mathrm{km}$ at 1550 nm. More details regarding the fiber laser can be found in Ref. [20]. Fundamentally, the laser produced soliton pulses at a repetition rate of 100 MHz, corresponding to a cavity round-trip time of 10 ns, when the laser pump power was set to ~100 mW. Although the laser could emit harmonically mode-locked (HML) solitons at higher pump power[20], we simply studied the fundamental state here for avoiding more complicated situations induced by redundant pump power. In order to regularly investigate the build-up processes of the laser, the pump light was modulated by an acoustic-optic modulator (AOM), which was driven by a square-wave signal at 0.4 Hz, produced from a radio-frequency waveform synthesizer (SMC100A, R&S). For spectral validation, a small portion of the laser output was sent to an optical spectrum analyzer (AQ6370D, Yokogawa). The rest was unevenly split into two parts. The smaller part was used for direct photodiode detection, tracking the pulse train in the time domain. The other was temporally stretched in a 5-km-long single-mode fiber (SMF) with a second-order dispersion of $-23\,\mathrm{ps}^2/\mathrm{km}$ at 1550 nm for TS-DFT measurements, where a high-speed digital oscilloscope (DSV334A, Keysight, bandwidth of 33 GHz at a sampling rate of 40 GSa/s) and a fast photodetector (bandwidth of 40 GHz) were used. Note that, before being launched into the SMF, the light was attenuated to about 0.6 mW for avoiding nonlinear effects.

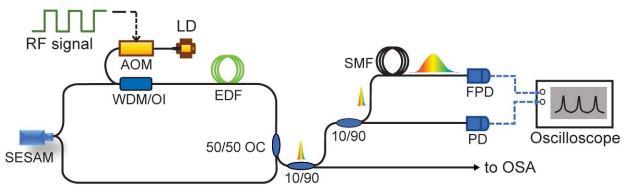

Fig. 1. Experimental setup. AOM, acoustic-optic modulator; LD, laser diode; EDF, erbium-doped fiber; OC, optical coupler; WDM/OI, wave division multiplexer and optical isolator; SMF, single-mode fiber; FPD, fast photo-detector; SESAM, semiconductor saturable absorber mirror; OSA, optical spectrum analyzer.

3. Results and Discussion

A portion of the data recorded in a TS-DFT measurement of 9.5 ms, corresponding to 0.95 million round trips, is shown in Fig. 2, presenting the formation and evolution of mode-locked fiber solitons. The spectra measured by TS-DFT (red) and the static spectrometer (black curve on a linear scale and green on a log plot) were consistent, as indicated in the inset of Fig. 2(a). Also, the typical Kelly sidebands were recognized for the soliton laser. The relation between the wavelength and the temporal spacing on the fast time scale was measured to be 5.5 nm/ns. Note that the spectral validation was carried out for a stationary ML state. Interestingly, unlike most demonstrated cases where noise and Q-ML occupied the stage prior to a stable ML state[9], a bunch of short-lived unstable multi-pulsing states were observed in our fiber laser. A zoom-in picture is displayed in Fig. 2(b). The states had short lifetimes [labeled as t_1 in Fig. 2(b)], varying from a few to nearly a hundred microseconds (μs). The separations of the states (t_2), however, were rather consistent, i.e., ~9 μs, likely determined by the gain recovery time of the laser system[21].

A transient pulsation state lasting 28 μs (or 2800 round trips) is displayed in Fig. 3(a). In order to investigate the spectral

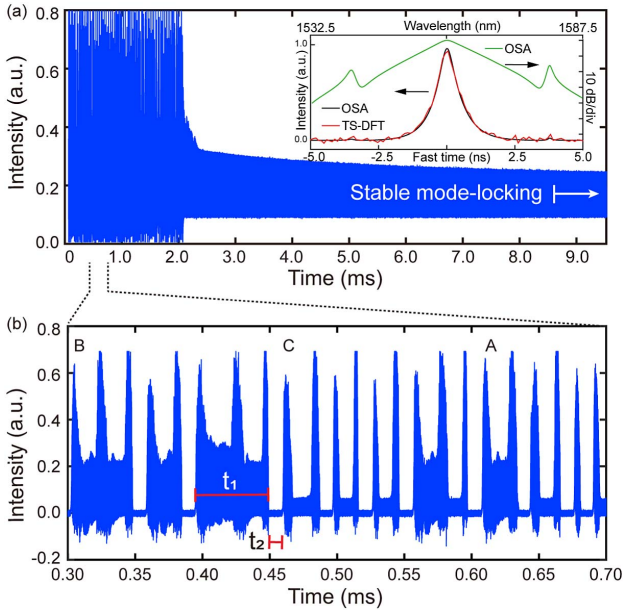

Fig. 2. (a) A time sequence recorded in a TS-DFT measurement. A build-up regime for the fiber laser is displayed. (b) Zoom-in picture of the regime prior to a stable ML state. Spectra measured by TS-DFT (single-shot) and OSA are displayed in inset of (a) and the OSA data are also plotted in log scale (green) for showing the Kelly sidebands. The states labeled as A, B, and C are presented in Figs. 3, 4, and 5, respectively.

dynamics, the TS-DFT data were rearranged into a two-dimensional (2D) map in Fig. 3(b) with consecutive round-trip numbers on the x axis and cavity round-trip time or fast time (i.e., 10 ns) on the y axis. Note that the corresponding wavelengths were not labeled in the 2D map, since the absolute values of the wavelength were unclear for the fast-changing, short-lived ML state.

Like a steady ML state[9,11], the raised RO stage, Q-ML, and beating dynamics were identified in the build-up of the transient ML state; unlike the steady state, the ML here was rather unstable, and the intra-cavity pulses quickly vanished after a short period of evolution (e.g., 12 μs or 1200 round trips in Fig. 3). A zoom-in picture of the spectral dynamics is displayed in Fig. 3(c). The interference pattern in the spectral domain, indicating multi-pulse interactions, was observed. For understanding the cause of such a pattern, each single-shot TS-DFT spectrum was Fourier transformed to reveal the field autocorrelation traces of the solitons. As a result, the temporal separations between the solitons were studied. Figure 3(d) shows complex pulse evolution dynamics, where multiple pulses coexisted, and the two strongest pulses [marked with arrows in Fig. 3(d)] repelled and then attracted each other, dominating the interference pattern with chirped frequencies in Fig. 3(c). The two pulses collided at the end of Fig. 3(d) and then merged into a single giant pulse with expanded spectral bandwidth [Fig. 3(b)], which quickly died out (e.g., within 2 μs).

The observed multi-pulse interactions (i.e., repulsion, attraction, and collision) in Fig. 3 were indeed a consequence of the balance between dispersion and nonlinearity[11–13] along with gain competition[22,23]. Also, as the intra-cavity energy was funneled into a single pulse, the intra-cavity nonlinearity was swiftly increased, causing notable spectral broadening in Fig. 3(b). Meanwhile, the sudden energy boost of the single pulse might cause significant gain depletion[21], which then led to decaying and eventually annihilation of the state. After that, the laser entered a stage of gain recovery [labeled as t_2 in Fig. 2(b)].

We also noticed that a whole decaying process might last a few μs or even longer, which was close to the recovery time of the gain. Hence, it was possible that the fiber laser was recovered from gain depletion before a pulsing state vanished completely. As a result, instead of annihilation, a new round of evolution might be initialized at the end of a decaying process. For instance, the decaying of a giant pulse in the middle of Fig. 4(a) led to formation of multiple pulses followed by another evolution process (from the 2900th to the 5000th round trip).

As evidenced by the spectral dynamics in Fig. 4(b), a spectral shift was noticed as a dislocation of the two evolving traces before and after the appearance of the giant pulse. In fact, due to the spectral dependency of intra-cavity loss, the decaying process was spectrally uneven. For instance, in our experiment, the long-wavelength components decayed much slower than the short wavelength ones, as shown in Fig. 4(b). Consequently, the former was more likely to survive from gain depletion and recovery, which also explained the red shift for the spectral evolution in Fig. 4(b).

Figure 5 shows another transient ML state in Fig. 2. Compared to the states in Figs. 3 and 4, the difference could be readily identified from the recorded time-domain trace in Fig. 5(a), where a train of relatively stable, low-intensity pulses were presented. Also, as indicated in the corresponding 2D spectral map [Fig. 5(b)], after RO and beating dynamics, two largely separated pulses were formed, each as a victor of multi-pulse competitions evidenced by the spectral interference patterns [corresponding to the round-trip numbers of 300 to 600 in Fig. 5(b)]. An expanded view of the spectral evolution of the two pulses is displayed in Fig. 5(c), together with a three-dimensional plot in Fig. 5(d). We noticed that the two evolving pulses were spectrally broadened while remaining separated, forming a short-lived bound state of pulses. In the end, one of the pulses led to a giant pulse, which terminated the ML due to gain depletion, and the other simply disappeared [shown in Fig. 5(b)] as a result of multi-pulse competition and energy balance[22]. A similar phenomenon was found in the decaying processes of a double-pulse ML fiber laser[23], where the laser pump power

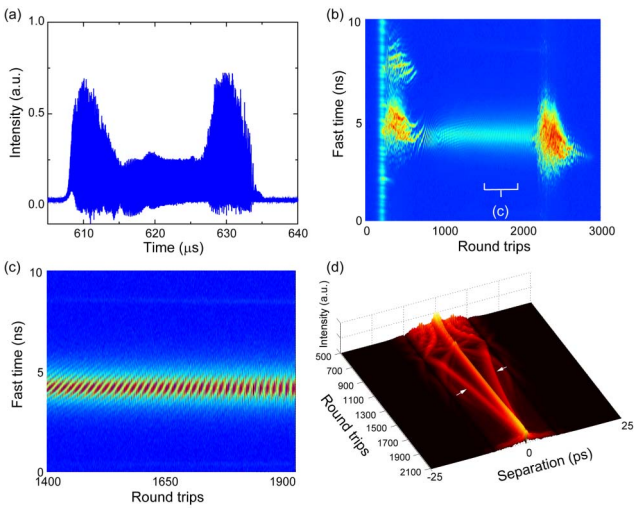

Fig. 3. (a) Time-domain sequence of a transient ML state and (b) the corresponding TS-DFT results displayed in a 2D map. (c) Zoom-in of (b) showing the spectral dynamics of the evolving pulses. (d) The field autocorrelation traces calculated with the Fourier transform of each TS-DFT spectrum in (b).

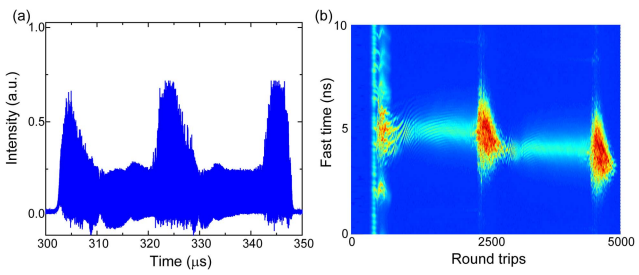

Fig. 4. (a) Time-domain trace and (b) real-time spectral evolution measured with TS-DFT for a transient ML state. The y axis from 0 to 10 ns corresponds to a spectral scale from longer to shorter wavelengths. Note that for the transient states, the absolute values of wavelengths were not determined.

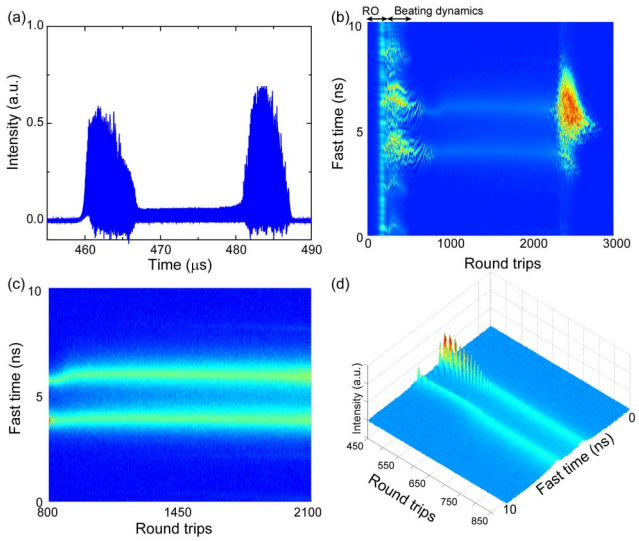

Fig. 5. (a) Recorded time-domain trace and (b) corresponding TS-DFT data for a different transient state. (c) An expanded view for the evolving solitons and (d) a three-dimensional image showing the spectral dynamics of the solitons.

was artificially reduced for triggering the decaying dynamics. Different from Ref. [23], our results showed that the double-pulse decay could occur in a transient ML regime, where the lasing dynamics were dominated by multi-pulse competition as well as gain depletion and recovery.

Furthermore, statistical analysis in Fig. 6(a) showed that the probability of occurrence for the transient ML states in Fig. 5 was 25%, defined by the event number of transient states normalized to the total one before the laser entered a stable ML regime. Comparatively, the probability for the case in Fig. 3 was about 10%. The results indicated that our laser tended to produce stably separated multiple pulses (like those in Fig. 5 or HML pulses in Ref. [20]). Also, when the pump power was further decreased by ~10%, nearly to the threshold of fundamental ML, only *Q*-switched bursts [each lasting less than 5 μs, as depicted in Fig. 6(b)] could be observed in the build-up stage. Such *Q*-switched lasing dynamics were similar to those in Ref. [9]. We believed that for our fiber laser, the excess pump power resulted in the transient and unstable ML states before the laser

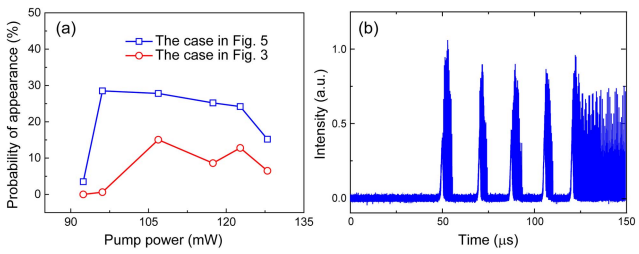

Fig. 6. (a) Probability of occurrence for two typical transient ML states observed with different pump powers, which correspond to the results presented in Figs. 3 and 5. (b) The time-domain trace recorded in the onset of the fiber laser with reduced pump power.

reached a point where intra-cavity energy, dispersion, and nonlinearity were balanced properly, and, consequently, a steady ML state could be achieved.

Our experimental observations showed that an unusual transient regime occurred before the build-up of a stable ML state in a fiber laser. The unambiguous presence of various transient ML states in this regime was revealed for the first time, to the best of our knowledge, which may enrich the existing dynamics during the development of the mode-locked pulses. Also, these behaviors might stimulate further theoretical analysis and numerical simulations to investigate the underlying mechanisms.

4. Conclusion

In conclusion, we observed a string of ML states with short life time varying from a few to nearly a hundred μs. Various lasing dynamics, including multi-pulse formation, interaction, and decaying evolution, were found in these transient states, all of which happened before a fiber laser reached a steady ML state. Furthermore, we found that redundant pump power or excess intra-cavity energy might be responsible for the emergence of these short-lived pulsing states. We believe these findings could be valuable for further studies of transient behaviors of mode-locked fiber lasers.

Acknowledgement

This work was supported by the National Key Research and Development Program (No. 2018YFB0504400), National Natural Science Foundation of China (NSFC) (Nos. 61875243 and 11804100), Shanghai Municipal Science and Technology Major Project (No. 2019SHZDZX01), and Science and Technology Innovation Program of Basic Science Foundation of Shanghai (No. 18JC1412000).

References

1. M. Horowitz, C. R. Menyuk, T. F. Carruthers, and I. N. Duling, "Theoretical and experimental study of harmonically modelocked fiber lasers for optical communication systems," J. Lightwave Technol. **18**, 1565 (2000).
2. T. Yang, H. Lin, and B. Jia, "Ultrafast direct laser writing of 2D materials for multifunctional photonics devices [Invited]," Chin. Opt. Lett. **18**, 023601 (2020).
3. M. E. Fermann and I. Hartl, "Ultrafast fibre lasers," Nat. Photon. **7**, 868 (2013).
4. M. Yan, L. Zhang, Q. Hao, X. Shen, X. Qian, H. Chen, X. Ren, and H. Zeng, "Surface-enhanced dual-comb coherent Raman spectroscopy with nanoporous gold films," Laser Photon. Rev. **12**, 1800096 (2018).
5. A. Mahjoubfar, D. V. Churkin, S. Barland, N. Broderick, S. K. Turitsyn, and B. Jalali, "Time stretch and its applications," Nat. Photon. **11**, 341 (2017).
6. G. Herink, F. Kurtz, B. Jalali, D.R. Solli, and C. Ropers, "Real-time spectral interferometry probes the internal dynamics of femtosecond soliton molecules," Science **356**, 50 (2017).
7. G. Herink, B. Jalali, C. Ropers, and D. R. Solli, "Resolving the build-up of femtosecond mode-locking with single-shot spectroscopy at 90 MHz frame rate," Nat. Photon. **10**, 321 (2016).

8. X. Liu and M. Peng, "Revealing the buildup dynamics of harmonic mode-locking states in ultrafast lasers," Laser Photon. Rev. **13**, 1800333 (2019).
9. R. Miao, M. Tong, K. Yin, H. Ouyang, Z. Wang, X. Zheng, X. Cheng, and T. Jiang, "Soliton mode-locked fiber laser with high-quality MBE-grown Bi_2Se_3 film," Chin. Opt. Lett. **17**, 071403 (2019).
10. X. Liu, D. Popa, and N. Akhmediev, "Revealing the transition dynamics from Q switching to mode locking in a soliton laser," Phys. Rev. Lett. **123**, 093901 (2019).
11. X. Liu, X. Yao, and Y. Cui, "Real-time observation of the buildup of soliton molecules," Phys. Rev. Lett. **121**, 023905 (2018).
12. J. Peng and H. Zeng, "Build-up of dissipative optical soliton molecules via diverse soliton interactions," Laser Photon. Rev. **12**, 1800009 (2018).
13. J. Peng, M. Sorokina, S. Sugavanam, N. Tarasov, D. V. Churkin, S. K. Turitsyn, and H. Zeng, "Real-time observation of dissipative soliton formation in nonlinear polarization rotation mode-locked fibre lasers," Commun. Phys. **1**, 20 (2018).
14. D. R. Solli, C. Ropers, P. Koonath, and B. Jalali, "Optical rogue waves," Nature **450**, 1054 (2007).
15. A. F. J. Runge, N. G. R. Broderick, and M. Erkintalo, "Observation of soliton explosions in a passively mode-locked fiber laser," Optica **2**, 36 (2015).
16. M. Liu, A. P. Luo, Y. R. Yan, S. Hu, Y. C. Liu, H. Cui, Z. C. Luo, and W. C. Xu, "Successive soliton explosions in an ultrafast fiber laser," Opt. Lett. **41**, 1181 (2016).
17. Y. Yu, Z. C. Luo, J. Kang, and K. K. Y. Wong, "Mutually ignited soliton explosions in a fiber laser," Opt. Lett. **43**, 4132 (2018).
18. K. Sulimany, O. Lib, G. Masri, A. Klein, M. Fridman, P. Grelu, O. Gat, and H. Steinberg, "Bidirectional soliton rain dynamics induced by Casimir-like interactions in a graphene mode-locked fiber laser," Phys. Rev. Lett. **121**, 133902 (2018).
19. G. Xu, A. Gelash, A. Chabchoub, V. Zakharov, and B. Kibler, "Breather wave molecules," Phys. Rev. Lett. **122**, 084101 (2019).
20. X. Wang, J. Peng, K. Huang, M. Yan, and H. Zeng, "Experimental study on buildup dynamics of a harmonic mode-locking soliton fiber laser," Opt. Express **27**, 28808 (2019).
21. J. N. Kutz, B. C. Collings, K. Bergman, and W. H. Knox, "Stabilized pulse spacing in soliton lasers due to gain depletion and recovery," IEEE J. Quantum Electron. **34**, 1749 (1998).
22. A. Komarov, H. Leblond, and F. Sanchez, "Multistability and hysteresis phenomena in passively mode-locked fiber lasers," Phys. Rev. A **71**, 053809 (2005).
23. G. Wang, G. Chen, W. Li, C. Zeng, and H. Yang, "Decaying evolution dynamics of double-pulse mode-locking," Photon. Res. **6**, 825 (2018).